Research Article

Kolade O. Faloye*#, Shaban Ahmad#, Olubunmi T. Oyasowo, Esther O. Shalom, Nagmi Bano, Esther A. Olanudun, Tawakalit O. Kelani, Habeeb E. Aliyu, Khalid Raza*, Boluwaji I. Makinde, Abdullah R. Alanzi*

Deciphering the influenza neuraminidase inhibitory potential of naturally occurring biflavonoids: An *in silico* approach

https://doi.org/10.1515/chem-2024-0053
received April 17, 2024; accepted June 1, 2024

Abstract: Influenza infection poses a significant threat to the existence of humans and animals. Its inhibition by secondary metabolites may proffer a lasting solution to its resistance to available synthetic therapeutic agents. In this study, we investigated the influenza neuraminidase (NA) inhibitory potential of naturally occurring C–O–C biflavonoids using integrated computational approaches. The molecular docking method was employed to identify biflavonoids with high binding affinities, and molecular dynamics simulation was performed for 100 ns to examine the stability, binding mode, and interactions elicited by the hit molecules in influenza NA-binding pocket. The bioavailability and pharmacokinetic properties of the hit biflavonoids were examined using swissADME. The molecular docking studies identified lophirone L, delicaflavone, lanaroflavone, pulvinatabiflavone, and ochnaflavone as the hit molecules with the binding affinity of −9.9 to −9.3 kcal/mol. The root means square deviation and root mean square fluctuation plots obtained from the molecular dynamics simulation showed that the selected biflavonoids were reasonably stable at the enzyme's binding pocket. The ADMET studies showed that the top-ranked biflavonoids exhibit good pharmacokinetic and bioavailability properties. Furthermore, the density functional theory studies showed that the selected hit secondary metabolite possesses good pharmacological properties. Thus, the inhibitory activities of these compounds on viral neuraminidase could be helpful in the management of influenza infections.

Keywords: influenza, influenza neuraminidase, molecular docking, molecular dynamics simulation, bioavailability

1 Introduction

Influenza is an acute respiratory infection caused by negative-stranded RNA influenza viruses and presents with significant complications like myocarditis, encephalitis, and multiple organ failure [1,2]. Influenza's life cycle has fundamental glycoproteins like neuraminidase (NA) and hemagglutinin (HA) [3]. The NA cleaves sialic acid residues on cellular receptors, thereby facilitating the release of newly produced virions, while HA binds to host cell receptors,

# These authors are equally contributed.

*** Corresponding author: Kolade O. Faloye,** Department of Chemistry, Faculty of Science, Obafemi Awolowo University, Ile-Ife 220282, Nigeria, e-mail: kollintonx1@gmail.com
*** Corresponding author: Khalid Raza,** Computational Intelligence and Bioinformatics Lab, Department of Computer Science, Jamia Millia Islamia, New Delhi 110025, India, e-mail: Kraza@jmi.ac.in
*** Corresponding author: Abdullah R. Alanzi,** Department of Pharmacognosy, College of Pharmacy, King Saud University, Riyadh, 11451, Saudi Arabia, e-mail: aralonazi@ksu.edu.sa
Shaban Ahmad, Nagmi Bano: Computational Intelligence and Bioinformatics Lab, Department of Computer Science, Jamia Millia Islamia, New Delhi 110025, India
Olubunmi T. Oyasowo: Department of Chemistry, Faculty of Science, Obafemi Awolowo University, Ile-Ife 220282, Nigeria
Esther O. Shalom: Drug Research and Production Unit, Faculty of Pharmacy, Obafemi Awolowo University, Ile-Ife 220282, Nigeria
Esther A. Olanudun: Department of Industrial Chemistry, Faculty of Science, University of Ilesa, Ilesa 5089, Nigeria
Tawakalit O. Kelani: Department of Chemistry, Faculty of Science, Obafemi Awolowo University, Ile-Ife 220282, Nigeria; Department of Chemical Sciences, Faculty of Science, Edo University, Iyamo 312107, Nigeria
Habeeb E. Aliyu: Department of Chemistry, Faculty of Science, Obafemi Awolowo University, Ile-Ife 220282, Nigeria; Department of Industrial Chemistry, Faculty of Science, University of Ilesa, Ilesa 5089, Nigeria
Boluwaji I. Makinde: Department of Biochemistry and Molecular Biology, Faculty of Science, Obafemi Awolowo University, Ile-Ife 220282, Nigeria
ORCID: Kolade O. Faloye 0000-0003-4992-2092; Khalid Raza 0000-0002-3646-6828; Shaban Ahmad 0000-0001-9832-2830

thereby promoting infection transmission [4,5]. In the 1970s, influenza NA was identified as a viable drug target which marked a crucial turning point in influenza-focused research [6]. Subsequent to the NA discovery, two standard drugs were developed for influenza management. The first neuraminidase inhibitor (NAI), zanamivir, was introduced, but its efficacy was hampered by a low absolute bioavailability [7,8]. Also, another NAI, oseltamivir was developed to address this bioavailability issue, but its use was limited by the resistance of influenza viruses to its therapeutic efficiency. The deficiencies of these drugs have promoted the search for novel therapeutic options characterized by good bioavailability and resistance mitigation [9,10].

Natural products are major sources of therapeutic agents and have proven effective against deadly diseases including viral and microbial infections [11–13]. Biflavonoids, also known as dimeric flavonoids, are polyphenolic secondary metabolites found in medicinal plants [14]. These plant-derived chemical compounds comprise those linked by a C–C or C–O–C bond between their phenyl-chromenone units (Figure 1) [15]. Biflavonoids connected via the C–O–C bond have shown remarkable pharmacological attributes like antioxidant, anti-inflammatory, anticancer, antiviral, antiparasitic, and hepatoprotective properties [15–18]. The major source of C–O–C biflavonoids include plants like *Rhus succedanea*, *Selaginella tamariscina*, *Lophira alata*, *Ginkgo biloba*, and *Campnosperma panamense* [19–23].

Computer-aided drug design is among the major innovative approaches developed to identify new drug leads that can effectively treat diseases [24]. Molecular docking is an efficient technique used to select a hit molecule through the prediction of its binding affinity against a disease target [24,25]. Molecular dynamic simulation is another method that helps to assess the stability, interactions of potential drug candidates, and their binding mode with specific target proteins [26]. Computational methods like molecular docking, molecular dynamics simulation, and density functional theory play a pivotal role in modern drug development. Several studies have established the efficacy of flavonoids and biflavonoids as potent antiviral agents [18,27,28]. However, the inhibitory property of naturally occurring C–O–C-linked biflavonoids is yet to be evaluated. Herein, we investigate the inhibitory potential of plant-derived C–O–C biflavonoids against influenza NA using integrated molecular docking and molecular dynamics simulation approaches.

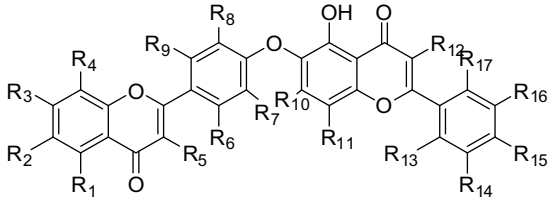

Figure 1: General structure of C–O–C-linked biflavonoids.

2 Methodology

We have plotted a graphical abstract in Figure 2 to show the methodology and how we proceeded with the analysis of targeting influenza with multiple C–O–C biflavonoids drugs. We successfully identified and probed their effectiveness in computational experimentations. Furthermore, the detailed methods are as follows.

2.1 Protein and ligand preparation

The 3D crystallographic structure of influenza NA (PDBID: 3TI5) [29] was retrieved from the protein data bank (www.rcsb.org) and loaded on PyMol software to remove the water molecules, co-factors, and ions. The native ligand (zanamivir) was also identified on PyMol software, and the residues within 5 Å resident at the protein binding site were selected. Later on, the native ligand was removed to obtain a clean protein. The protein was saved in a PDB format for docking purposes.

The chemical structures of the 20 naturally occurring C–O–C biflavonoids (see supplementary material, Table S1) were built with Spartan 14 software, while the standard drugs (zanamivir and oseltamivir) were downloaded from the PubChem database (https://pub-chem.ncbi.nlm.nih.gov/). All the chemical structures were saved in an SDF format and loaded into Open Babel for energy minimization. Then, the energy-minimized ligands were saved in PDBQT format.

2.2 Molecular docking studies

The docking methodology was first validated by re-docking the native ligand in the binding pocket of influenza NA and estimating its root means square deviation (RMSD) value. The molecular docking studies of the C–O–C biflavonoids, zanamivir and oseltamivir, against influenza NA were done by converting the clean protein's PDB file to PDBQT using the MGL software. After that, the protein was loaded into the Autodock Vina interface of PyRx 0.8 software [30]

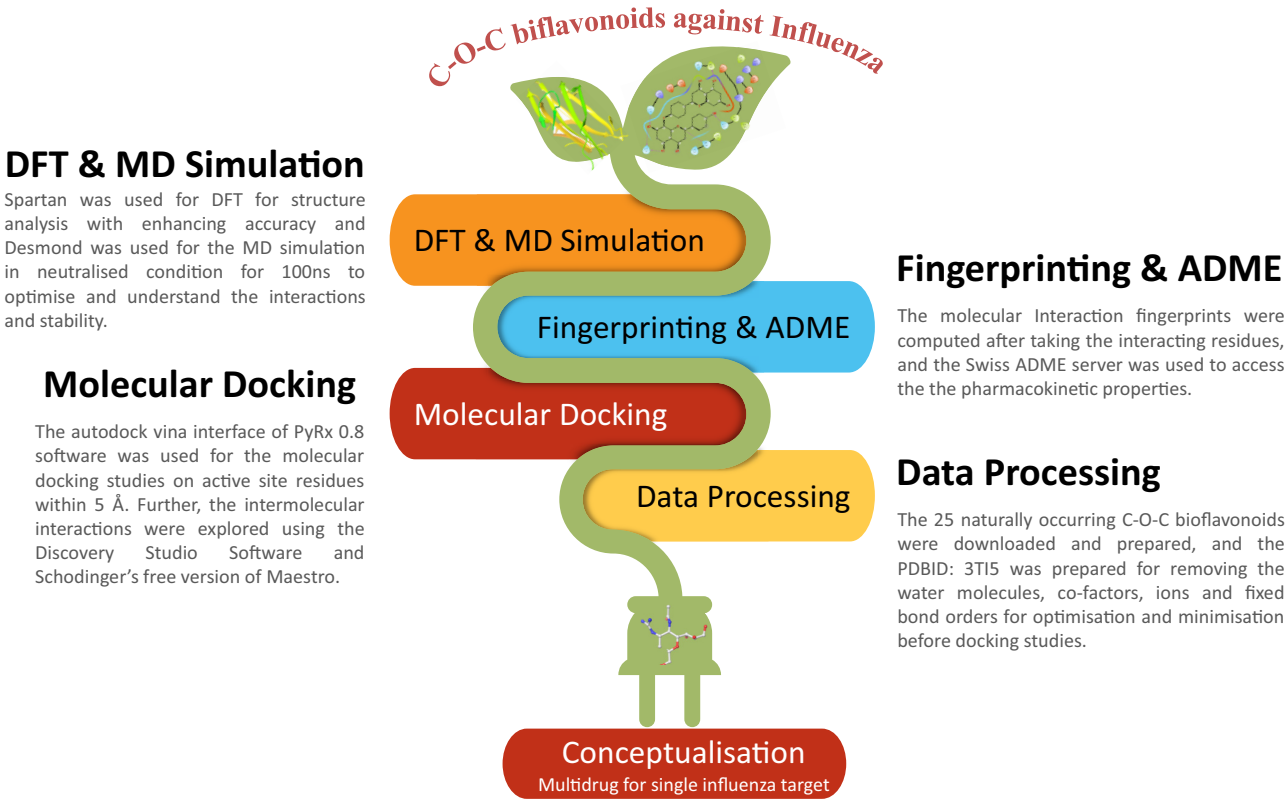

Figure 2: Showing the graphical abstract of the study from conceptualization to identifying and validation using the computational approaches.

and amino acid residues (Arg118, Glu119, Leu134, Arg151, Arg152, Arg156, Trp178, Ser179, Ile222, Arg224, Glu227, Ser246, Glu276, Glu277, Arg292, Asn294, Gly348, Arg371, Tyr406) resident within 5 Å was selected. Then, the grid box of the protein was adjusted to center_x = 66.2633, center_y = 15.9425, and center_z = −0.7511 and size_x = 27.3432, size_y = 17.5309, and size_z = 25.8509. The PDBQT file of the biflavonoids, zanamivir and oseltamivir, was loaded, and molecular docking was carried out against influenza NA at an exhaustiveness of 100. After successfully completing the docking procedure, the binding poses of the ligand were retrieved, and those with the lowest RMSD value were selected for hydrogen bonding, hydrophobic, and pi-interaction analysis using the Discovery Studio Visualizer software.

2.3 Molecular interaction fingerprints (IFP) and pharmacokinetic studies

The molecular IFP was computed using the IFPs tool in Schrödinger Maestro, where we selected each complex, checked the receptor–ligand complex option, and kept to any contact types. We directly computed the fingerprints as the protein was the same, so it was unnecessary to align the sequences. Any contact type and color main plot were kept to make it clearer, and it was further enhanced by keeping only interacting residues, and the ligand display property was kept to the docking score to interpret it better [31–33]. Furthermore, the pharmacokinetic properties of the potential influenza NAIs were assessed using the SwissADME (http://www.swissadme.ch/) and pkCSM (http://www.biosig.lab.uq.edu.au/pkcsm/) online servers. Parameters such as solubility, human intestinal absorption, hepatotoxicity, bioavailability, and the secondary metabolites' carcinogenic properties were considered to understand their druggable potentials.

2.4 Density functional theory studies

In drug design, density functional theory (DFT) stands for density functional theory, a computational quantum mechanical method used to study the electronic structure of molecules. DFT analysis helps us understand how electrons are distributed in a molecular system, providing crucial insights into various molecular properties, and in drug designing, DFT is employed to delve into the energetics and electronic properties of drug molecules and their interactions with target proteins. We can gain insights into potential drug candidates' stability, reactivity, and binding affinity

by calculating electronic densities and energy levels. DFT analysis allows us to predict molecular properties such as molecular orbitals, electron density distribution, and electrostatic potential. These predictions are vital for understanding how drugs behave at the molecular level. The DFT calculations of the hit secondary metabolites were performed with the Spartan 14 program using functional B3LYP with a 6-31G basis set [34]. In these calculations, the frontier orbital parameters like energy gap (ΔE_{gap}), chemical reactivity (μ), electrophilicity index (ω), and electronegativity (χ) were estimated.

$$\Delta E_{gap} = E_{LUMO} - E_{HOMO}, \quad (1)$$

$$\mu = \frac{1}{2}(E_{HOMO} + E_{LUMO}), \quad (2)$$

$$\omega = \frac{\mu^2}{2\eta}, \quad (3)$$

$$\chi = -\mu. \quad (4)$$

2.5 Molecular dynamic (MD) simulation

The MD simulations of the docked complexes were performed using the academic version of DE Shaw's Desmond [35]. The system builder tool was used to prepare the system model in which we have used the SPC water model in orthorhombic conditions with 10 × 10 × 10 Å distances in buffer conditions. $3Na^+$ was added to each complex to neutralize the system as all of them had the net charge of −3 and then excluded ion and salt placement within 20 Å before minimization of volume to have a properly fitted neutralized system. Furthermore, the OPLS4 forcefield was used to minimize the complete system. The MD simulation was performed using the molecular dynamic panel for 100 ns with a recording interval of 100 ps that generated a total of 1,000 frames at 300 K temperature with 1.01325 bar pressure and was kept in the NPT ensemble to produce the trajectories that were further analyzed with the simulation interaction diagram tool [36,37].

3 Results

3.1 Molecular docking studies

The docking methodology adopted for the study was validated, and an RMSD value of less than 2 was obtained, indicating that the method developed is reproducible. The docking studies explored the ligand with the favorable binding affinity with the active binding site of influenza NA. The result revealed that all selected hit molecules displayed excellent docking scores ranging from −9.3 to −9.9 kcal/mol compared to zanamivir and oseltamivir that elicited the binding affinity of −7.9 and −6.1 kcal/mol as shown in Table 1.

Table 1: Interaction analysis of the hit biflavonoids against influenza NA

Ligand	Binding energy kcal/mol	Hydrogen bond		Hydrophobic interaction	Pi-interaction	Electrostatic interaction
		Amino acid	Distance (Å)			
Lophirone L	−9.9	Glu227	2.1238	Arg224, Arg371, Ile421, Pro431, Lys432	Arg224, Arg371, Ile421, Pro431, Lys432	Asp151, Arg292, Arg371
		Arg292	2.6414			
		Arg371	1.9069			
		Arg371	2.0590			
		Arg371	2.0902			
		Trp406	2.4209			
		Trp406	2.8049			
Delicaflavone	−9.6	Trp178	2.4947	Arg224, Arg371, Pro431	Arg224, Arg371, Pro431	Asp151, Glu277, Arg371
		Ser370	2.4658			
Lanaroflavone	−9.5	Trp178	2.3234	Ile149, Arg224, Pro431	Ile149, Arg224, Pro431	Arg118, Glu277, Arg371
		Asn347	1.9884			
Pulvinatabiflavone	−9.4	Ser246	2.3614	Arg371, Ile427, Pro431, Lys432	Arg371, Ile427, Pro431, Lys432	Glu276, Arg371
		Arg292	2.9499			
		Ile427	2.7219			
Ochnaflavone	−9.3	Ser246	2.1059	Pro236, Arg371, Ile427, Pro431, Lys432	Pro236, Arg371, Ile427, Pro431, Lys432	Glu276, Arg371
		Glu277	2.1095			
		Arg292	2.5537			
		Arg371	2.4347			

Lophirone L isolated from *L. alata* leaves elicited the best binding affinity against influenza NA at −9.9 kcal/mol. The hydrogen atoms on the biflavonoid established good hydrogen bond interaction with Glu227 at 2.1238 Å, Arg371 at 1.9069 Å, and Trp406 at 2.4209 and 2.8049 Å. Also, the oxygen atoms on the phytochemical moiety formed hydrogen bonds with Arg292 at 2.6414 Å, Arg371 at 2.0590 and 2.0902 Å, and Trp406 at 1.9069 Å, respectively. It was further stabilized at the influenza NA binding site by participating in hydrophobic and pi-interactions (pi-alkyl) with Arg224, Arg371, lle427, Pro431, and Lys432. Furthermore, electrostatic interactions were observed between the ligand and amino acid residues like Asp151, Arg292, and Arg371 (Figure 3c, Table 1). Delicaflavone obtained from *L. alata* was identified as the second-best ligand with a binding affinity of −9.6 kcal/mol. The hydrogen atoms on the delicaflavone moiety participated in hydrogen bond interactions with Tyr178 at 2.4947 Å and Ser370 at 2.4658 Å. The polyphenolic phytochemical was further stabilized at hydrophobic and pi-interactions (pi-alkyl) with Arg224, Arg371, and Pro431. Also, electrostatic interactions were established between the amino acid residues resident at the active site of the hit biflavonoid and Asp151, Glu277, and Arg371 (Figure 3a, Table 1). Lanaroflavone isolated from *C. panamense* was selected as the third-best hit phytochemical against the enzyme, with a binding affinity of −9.5 kcal/mol. The potential influenza NAI established hydrogen bond interactions with Trp178 at 2.3234 Å and Asn347 at 1.9884 Å. Also, the ligand attained stability at the enzyme's binding pocket by forming hydrophobic and pi-interactions with Ile149, Arg224, and Pro431. Additionally, electrostatic interactions were observed between the ligand and Glu276 and Arg371 (Figure 3b, Table 1). Pulvinatabiflavone obtained from *S. tamariscina* elicited a binding affinity of −9.4 kcal/mol and was selected as the fourth-best-hit molecule. The oxygen and hydrogen atoms on the polyphenolic phytochemical participated in hydrogen bond interaction with Arg292 at 2.9499 Å, Ser246 at 2.3614 Å, and Ile427 at 2.7219 Å. Pulvinatabiflavone was stabilized at the influenza NA binding pocket by forming hydrophobic and pi-interactions with Arg371, Ile427, Pro431, and Lys432. Furthermore, electrostatic interactions were identified between the phytochemical and Glu276 and Arg371, respectively (Figure 3e, Table 1). Ochnaflavone isolated from *Ochna pretoriensis* was selected as the fifth-best influenza NAI as it gave a binding affinity of −9.3 kcal/mol. The oxygen and hydrogen atoms on the hit biflavonoid formed hydrogen bond interactions with Arg292 at 2.5537 Å, Ser246 at 2.1059 Å, Arg371 at 2.4347 Å, and Glu277 at 2.1095 Å. Ochnaflavone was further

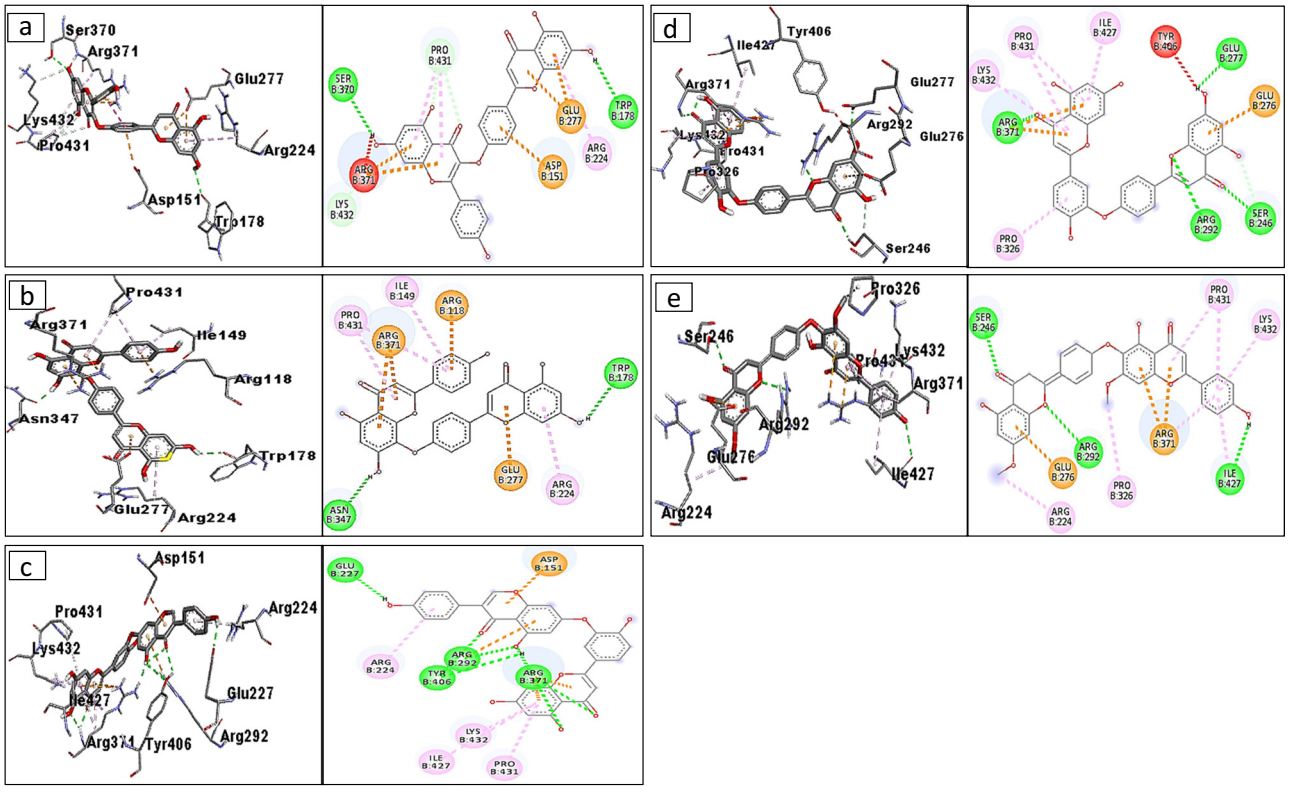

Figure 3: Showing the docked pose in 3D and 2D for 3TI5 with (a) delicaflavone, (b) lanaroflavone, (c) lophirone, (d) ochnaflavone, and (e) pulvinatabiflavone.

stabilized by participating in hydrophobic and pi-interactions with Pro236, Arg371, Ile427, Pro431, and Lys432. Also, electrostatic interactions were observed between the polyphenolic compound and Glu276 and Arg371 (Figure 3d, Table 1).

3.2 Molecular IFP and pharmacokinetic analysis

Molecular IFP is a computational method that encodes molecular interactions. Its importance lies in characterizing and comparing ligand–receptor interactions, aiding drug discovery by predicting binding affinities, and understanding structure–activity relationships, which are crucial for designing effective pharmaceuticals with desired therapeutic outcomes. The molecular IFP played a pivotal role in refining our understanding of ligand–receptor interactions. It validated the most interacting residues obtained from docking results, revealing a nuanced landscape. Notably, the counts for specific residue types were as follows: 20 for ARG (arginine), 11 for ASN (asparagine), 5 for ASP (aspartic acid), 16 for GLU (glutamic acid), 1 for GLY (glycine), 7 for ILE (isoleucine), 2 for LYS (lysine), 2 for PRO (proline), 11 for SER (serine), 5 for TRP (tryptophan), and 5 for TYR (tyrosine) (Figure 4). This detailed information on interacting residues enhances the precision of drug design efforts by highlighting key amino acids involved in crucial binding interactions. The pharmacokinetic properties of the top-ranked biflavonoids were assessed, and the results obtained are presented in Table 2. All the potential influenza NAIs violated Lipinski's rule of 5 and did not exhibit AMES toxicity, carcinogenicity, or hepatotoxicity features. The solubility of a drug candidate that ranges between −6.5 and 0.5 is acceptable in drug discovery and design [38]. The assessment showed that all the chemical compounds possess similar solubility potential with values ranging from −2.895 to −2.974, compared to zanamivir (−2.892) and oseltamivir (−2.029). Also, an acceptable value for a drug candidate's human intestinal absorption property is greater than 30. In this study, all the secondary metabolites possess good human intestinal absorption properties with values ranging from 76.411 to 99.200 compared to zanamivir (3.951) and oseltamivir (79.326). Furthermore, the bioavailability property of the top-ranked secondary metabolites was compared with that of zanamivir and oseltamivir. All the hit biflavonoids elicited the same bioavailability value of 0.55, while zanamivir gave 0.17 and oseltamivir gave 0.55.

3.3 Frontier molecular orbital properties of the top-ranked secondary metabolites

The structures of lophirone L, delicaflavone, lanaroflavone, pulvinatabiflavone, and ochnaflavone were

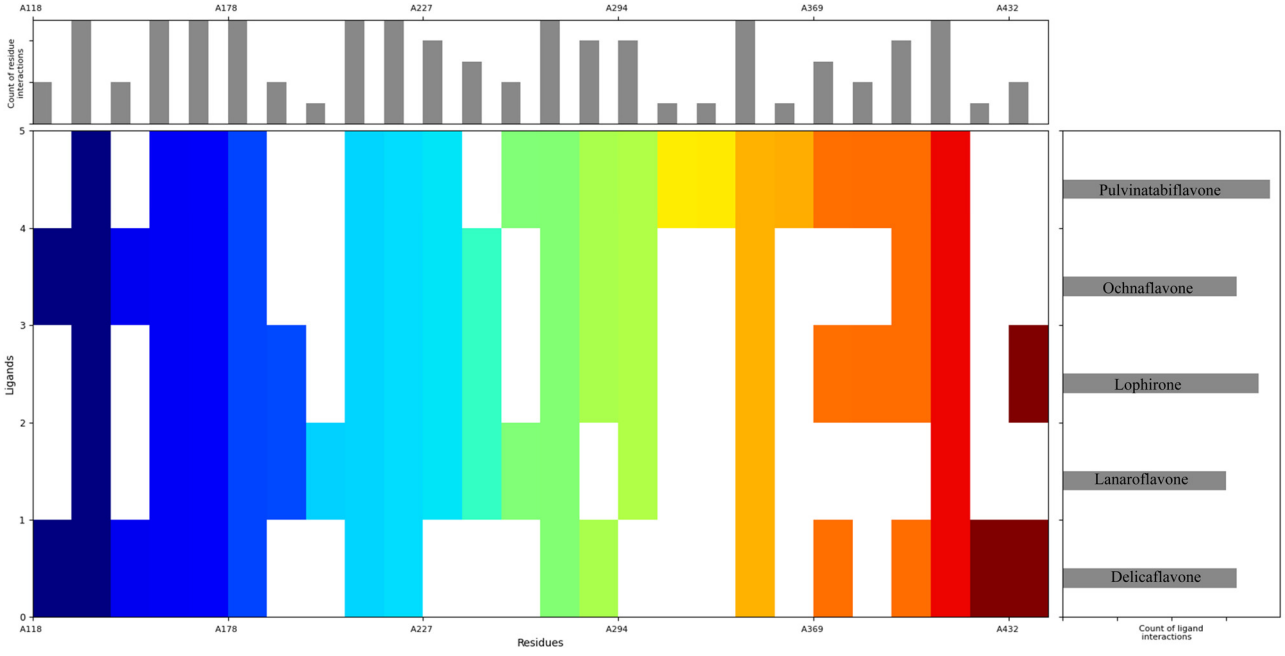

Figure 4: Showing the molecular IFPs of the docked poses of each compound.

Table 2: Pharmacokinetic properties of top-ranked biflavonoids

Ligands	Lipinski violation	Solubility	Human intestinal absorption	Hepatotoxicity	Carcinogenicity	Bioavailability score
Lophirone L	1	−2.93	86.135	–	–	0.55
Delicaflavone	1	−2.908	81.282	–	–	0.55
Lanaroflavone	1	−2.93	76.411	–	–	0.55
Pulvinatabiflavone	1	−2.97	99.2	–	–	0.55
Ochnaflavone	1	−2.974	90.304	–	–	0.55
Zanamivir	0	−2.892	3.951	–	–	0.17
Oseltamivir	0	−2.029	79.326	–	–	0.55

optimized, as shown in Figure 5. The energy of the highest occupied molecular orbital (E_{HOMO}) of a secondary metabolite indicates its ability to act as an electron donor, while the energy of the lowest unoccupied molecular orbital (E_{LUMO}) helps to understand the electron accepting capacity of a secondary metabolite [39,40]. Lophirone L elicited the highest E_{HOMO} value, indicating it as the best electron-donating molecule among the potential influenza NAIs. Also, lanaroflavone gave the lowest E_{LUMO} value, suggesting that it is the best electron-accepting phytochemical (Table 3).

A secondary metabolite's energy gap (ΔE_{gap}) provides relevant information about its pharmacological potential, chemical reactivity, and stability [41]. In this study, the stability of the secondary metabolites is in the order of delicaflavone > ochnaflavone > pulvinatabiflavone > lophirone L > lanaroflavone. Also, lanaroflavone was ranked as the secondary metabolite with the best reactivity potential, and other top-ranked secondary metabolites are in the order of lophirone L > pulvinatabiflavone > ochnaflavone > delicaflavone.

Electronegativity is an essential property that helps understand secondary metabolites' electron acceptability potential [42]. It also gives an idea of the bioactive potentials of the chemical compound. A high electron acceptability of a secondary metabolite signifies its high calculated electronegativity value [43]. Lophirone L gave the highest electronegativity value, indicating that the secondary metabolites exhibit good electron-accepting properties. Also, the electrophilicity index of secondary metabolites elucidates their pharmacological potential and potency against different diseases. A higher electrophilicity index value corresponds to a stronger electrophilic property [26]. The electrophilicity of the secondary metabolites is in the order of lanaroflavone > ochnaflavone > lophirone L > delicaflavone > pulvinatabiflavone. The frontier molecular orbital properties of selected influenza NAIs are presented in Table 3.

3.4 Molecular dynamic simulation analysis

Molecular dynamic simulation was performed on the protein-ligand complexes of the potential influenza NAIs previously identified in the molecular docking studies to understand their stability, binding mode, and interactions. The RMSD plot of the 3TI5-isophorone L complex showed that stability was attained from 0 to 14 ns, while consistent deviation was observed from 15 to 100 ns. The influenza NA's root mean square fluctuation (RMSF) plot swung between 0.4 and 2.7 Å (Figure 6). The contact plot analysis showed that good water bridge interactions were formed with Arg118, Ile149, Lys150, Asp151, Arg152, Ser153, Tyr155, Arg156, Trp178, Gly196, Ser270, Glu276, and Asn344, while hydrophobic interaction was observed with Arg156. Also, hydrogen bond interaction was observed between lophirone L and Asp151, Arg152, Glu276, and Asn344 (Figure 6). The RMSD plot of the 3TI5-delicaflavone complex showed that stability was obtained from 0 to 56 ns, while slight deviation was observed between 57 and 62 ns and became stable from 63 to 78 ns. However, consistent deviation was observed from 79 to 100 ns (Figure 6). Also, the RMSF plot showed that the protein swung between 0.4 and 3.2 Å throughout the 100 ns simulation period. The interaction analysis showed that Asn88, Arg118, Lys150, Asp151, Arg152, Asn234, Lys264, Glu276, Glu286, Arg292, Ala346, and Ser370 formed water bridge with delicaflavone. Also, hydrogen bond interactions between the hit biflavonoid and Lys150, Asp151, Glu276, and Ala346 were observed. However, no hydrophobic interaction was observed between the ligand and influenza NA (Figure 7). The analysis of the RMSD plot of 3TI5-lanaroflavone showed that the ligand was stable at the binding pocket of influenza NA between 5 and 58 ns, while slight deviation was observed between 59 and 61 and attained stability from 62 to 100 ns. The RMSF plot of the protein oscillated between 0.5 and 3.5 Å (Figure 6). The interactions obtained from the contact plot showed that good water bridge interaction formed between Glu119,

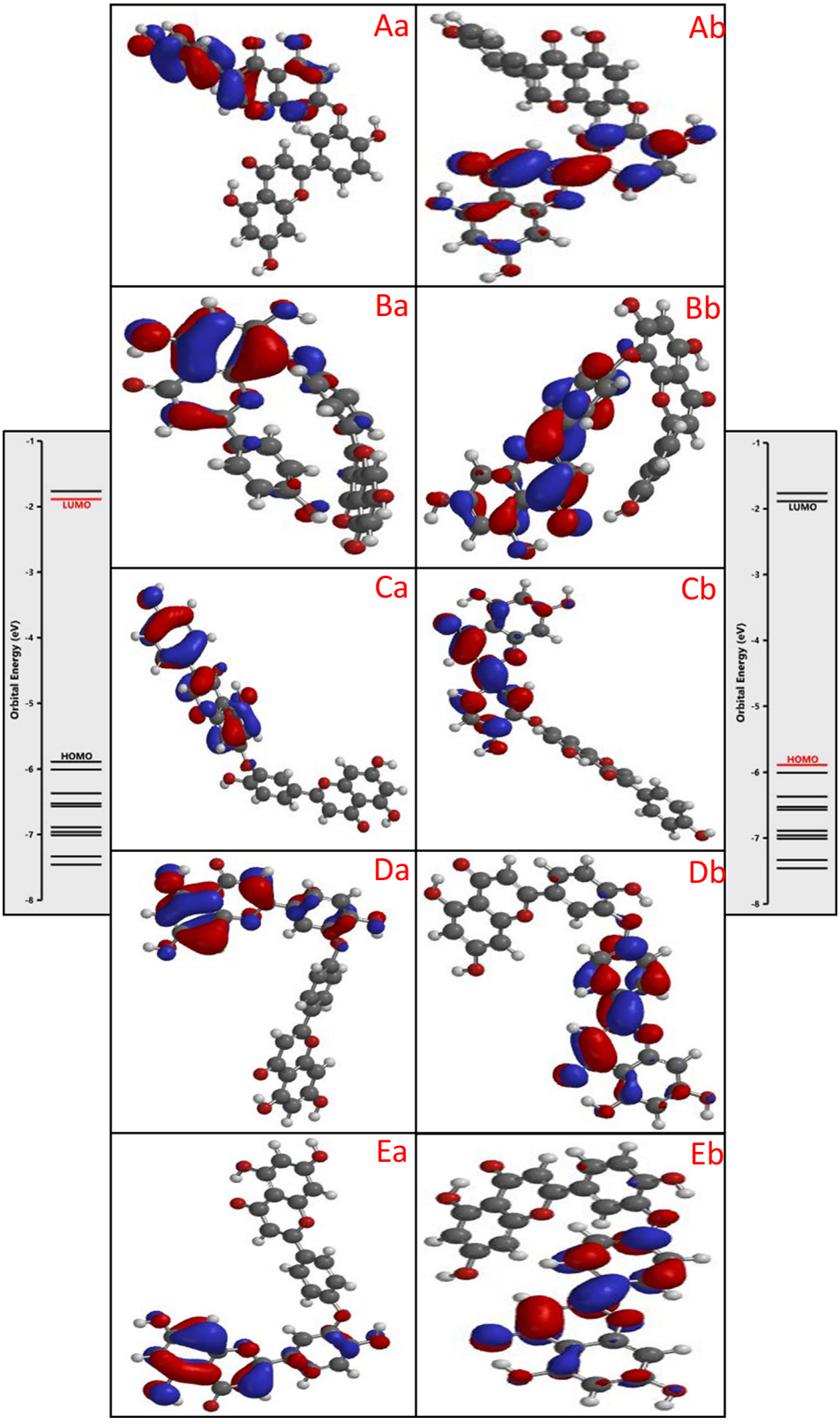

Figure 5: Showing the DFT computations-based HOMO diagram of (Aa) delicaflavone, (Ba) lanaroflavone, (Ca), lophirone, (Da) ochnaflavone, and (Ea) pulvinatabiflavone and LUMO diagram of (Ab) delicaflavone, (Bb) lanaroflavone, (Cb) lophirone, (Db) ochnaflavone, and (Eb) pulvinatabiflavone.

Table 3: Calculated frontier molecular orbital properties of selected biflavonoids

Ligands	E_{HOMO} (eV)	E_{LUMO} (eV)	ΔE_{gap} (eV)	μ (eV)	χ (eV)	ω (eV)
Lophirone L	−5.72	−1.90	3.89	3.81	3.80	−3.81
Delicaflavone	−5.89	−1.89	4.00	3.89	3.78	−3.89
Lanaroflavone	−5.91	−2.25	3.66	4.08	4.54	−4.08
Pulvinatabiflavone	−5.86	−1.76	3.89	3.91	3.53	−3.91
Ochnaflavone	−6.01	−2.02	3.99	4.02	4.05	−4.02

ΔE_{gap} = energy gap; μ = chemical potential; χ = electronegativity; ω = electrophilicity index.

Lys150, Asp151, Arg152, Ser153, Arg156, Trp178, Asn221, Glu227, Ser246, Asn247, Glu277, Asn294, and Asn347. Also, hydrogen bond interactions were identified between Ser153, Ser247, Glu277, and Asn294 (Figure 7). The RMSD plot of 3TI5-pulvinatabiflavone showed that the hit biflavonoid was stable with a slight deviation from 0 to 79 ns, followed by a deviation between 80 and 95 ns and stability from 96 to 100 ns (Figure 6). The RMSF plot showed that the protein oscillated between 0.4 and 2.4 Å throughout the 100 ns simulation period (Figure 6). The interaction analysis performed on the contact plot of the simulated 3TI5-pulvinatabiflavone showed that water bridge interaction was observed between the ligand and Arg152, Glu277, Arg292, and Arg371, while hydrogen bond interactions were observed with Tyr178 and Glu227 (Figure 7). The 3TI5-ochnaflavone RMSD plot showed stability between 0 and 19 ns, followed by slight fluctuations between 20 and 39 ns. The complex became stable with slight fluctuation from 40 to 86 ns, followed by consistent deviation from 87 to 100 ns (Figure 6). The RMSF plot showed that the protein oscillated between 0.4 and 2.7 Å (Figure 6). The contact plot analysis showed that water bridge interactions were established between Glu119, Asp151, Arg152, Trp178, Glu277, Arg292, Asn294, Asn347, Arg371, and Arg430. Furthermore, hydrogen bond interactions between Arg118, Arg152, Tyr178, Glu277, Asn294, Asn325, Asn347, and Arg371 were observed (Figure 7).

4 Discussion

Influenza is a communicable acute respiratory infection caused by the influenza virus in humans. This infection presents with various episodes of nose, throat, and lung problems and can sometimes lead to death when left untreated [3,44]. The influenza NA enzyme breaks sialic acid groups from cell glycoproteins, releasing the virus from host cells [45]. It facilitates the binding of viruses to the sialic acid groups of cell glycoproteins, which enhances the role of HA in binding receptors, improving the enzyme activities of NA, and facilitating virus infection in their respective hosts [46–48]. Hence, inhibiting the enzyme can drastically reduce or eradicate the replication of the virus. Biflavonoids are naturally occurring polyphenolic compounds that display huge varieties of pharmacological activities, including antiviral, hepatoprotective, anticancer, and anti-inflammatory [15,17]. Though there are two forms of biflavonoids, the C–O–C type biflavonoids are known for some attractive therapeutic potentials due to the combination of two flavonoid moieties [15]. Drug discovery and design through computational methods have been identified as faster, cheaper, and efficient alternatives, especially when there is an urgent need for a new therapeutic arsenal to treat or manage the outbreak of an ailment [26]. In this study, molecular docking studies identified lophirone L, delicaflavone, lanaroflavone, pulvinatabiflavone, and ochnaflavone as the potential influenza NAIs with good binding affinities compared to zanamivir. All the hit molecules established good hydrogen bonds and hydrophobic, pi, and electrostatic interactions with the amino acid residues at the active site of influenza NA. These interactions contribute to the good binding affinity, inhibitory potential, and stability elicited by the hit C–O–C type biflavonoids against the influenza NA enzyme.

The molecular dynamics simulation studies showed that most of the hit biflavonoids selected attained stability with slight fluctuations observed throughout the 100 ns simulation period. The RMSD and RMSF plots of protein–ligand complexes provide relevant information on the stability of the ligand at the protein's binding pocket and the dynamic behavior of the phytochemical with the influenza NA enzyme throughout the 100 ns simulation period [26]. In terms of stability, the ligands were reasonably stable throughout the simulation period, indicating that they can effectively inhibit influenza NA.

The contact plot of the protein–ligand complexes showed that the hit C–O–C biflavonoids formed important water bridges, hydrogen bonds, and hydrophobic interactions, which are incredibly relevant to their drug candidacy. Hydrogen bonds are crucial in protein–ligand binding,

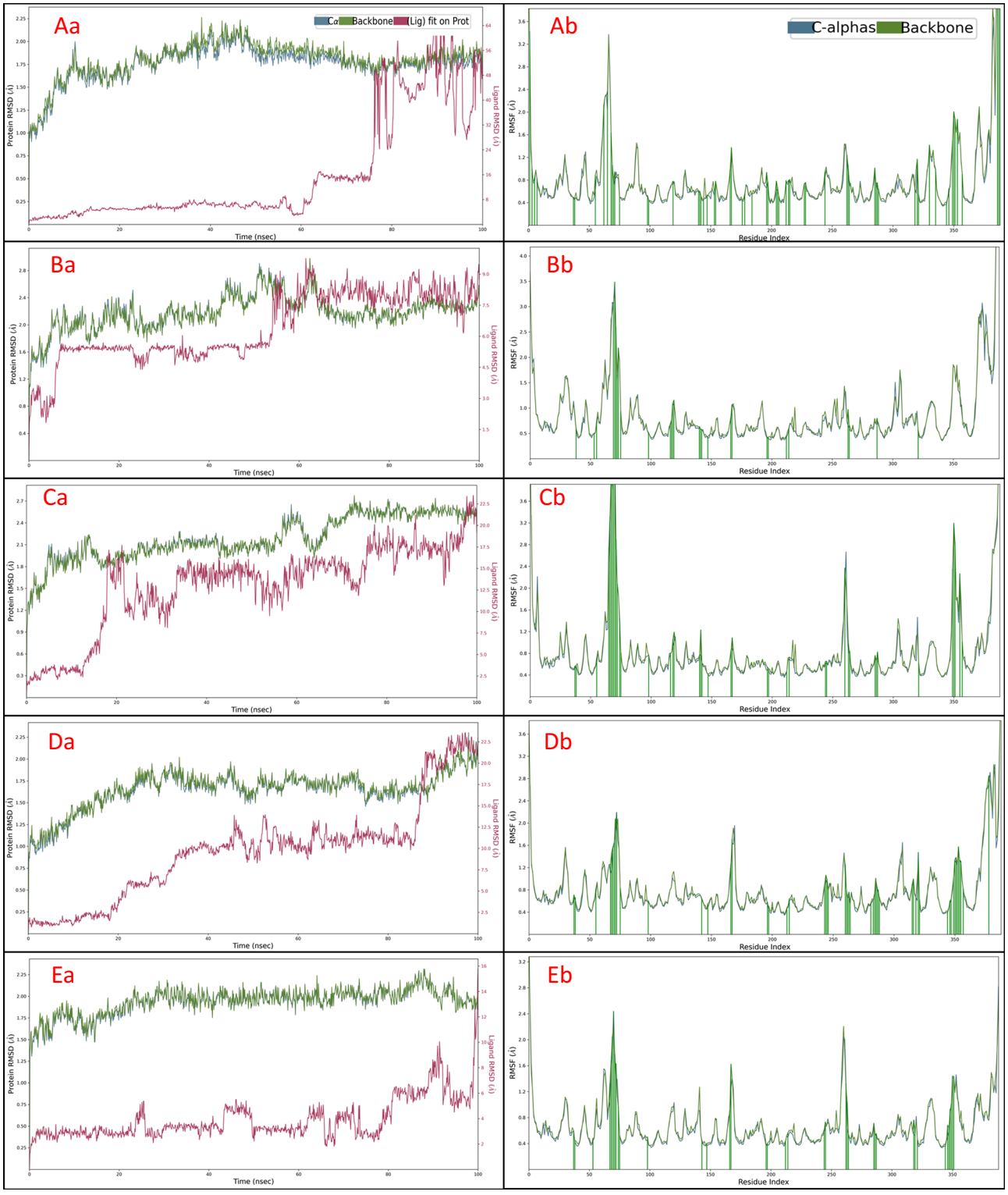

Figure 6: Showing the RMSD of 3TI5 (blue-Cα, green backbone) in complex with (Aa) delicaflavone, (Ba) lanaroflavone, (Ca) lophirone, and (Da) ochnaflavone, (Ea) pulvinatabiflavone in red color. The RMSF of 3TI5 (blue-Cα, green backbone) in complex with (Ab) delicaflavone, (Bb) lanaroflavone, (Cb) lophirone, (Db) ochnaflavone, and (Eb) pulvinatabiflavone where the interaction of the protein with ligand residues is shown in green lines.

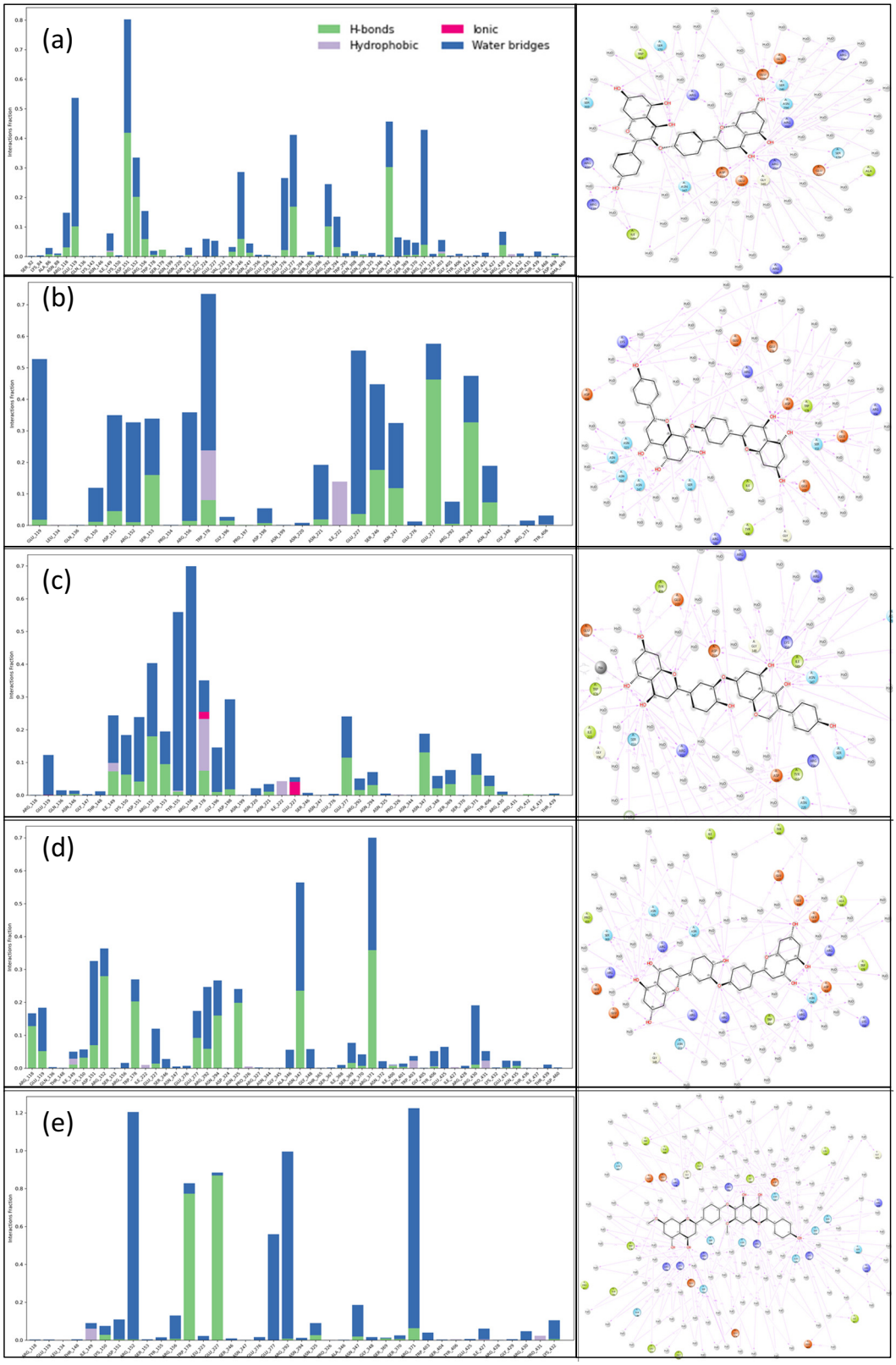

Figure 7: Showing the simulation interaction diagram of 3TI5 in complex with (a) delicaflavone, (b) lanaroflavone, (c) lophirone L, (d) ochnaflavone, and (e) pulvinatabiflavone where we have shown the interactions and histogram for the count of interactions.

absorption, and metabolism of drug candidates. These phytochemicals' ability to establish hydrogen bonds in the simulated system showed that they may quickly be metabolized when taken into the biological system to treat the influenza virus. Furthermore, the hydrogen bond formation with the influenza NA residues may have resulted from the abundance of hydroxyl and carbonyl groups on the biflavonoids. The huge water bridge formation between the hit biflavonoids and the enzyme showed that they could efficiently metabolize and interact extensively with the amino acid residues at the enzyme's binding site.

The pharmacokinetic prediction assessed the hit secondary metabolites' solubility, human intestinal absorption, bioavailability, hepatotoxicity, and carcinogenicity properties. All the chemical compounds that demonstrated good inhibitory potential against influenza NA exhibit good solubility and human intestinal absorption properties similar to oseltamivir and better than zanamivir. The top-ranked inhibitors showed a good bioavailability score compared to zanamivir and were considered non-carcinogenic compounds and non-toxic to the liver. Also, the frontier molecular orbital properties of the hit secondary metabolites showed that they exhibit good pharmacological properties.

Several studies have identified the C–O–C biflavonoids as good antiviral, antibacterial and antimicrobial agents [15]. The hit biflavonoids comprise two flavonoid units mainly dominated by luteolin and apigenin moieties. Several reports have established the excellent efficacy of the flavonoid units as potent antiviral agents [27,49–51]. Vacca et al. [52] evaluated some selected flavonoids' *in silico* NAI properties and ranked apigenin as one of the hit molecules with a binding affinity lower than those obtained for the C–O–C biflavonoids. Hence, the presence of two flavonoid units in the potential influenza NAIs identified in this study may have contributed to their high binding affinities, such that they have a higher possibility of working synergistically with each other.

5 Conclusion

The study examined the influenza NAI potential of naturally occurring C–O–C biflavonoids. A molecular docking study was conducted to select potential drug candidates against the target receptor. Lophirone L, delicaflavone, lanaroflavone, pulvinatabiflavone, and ochnaflavone were identified as new therapeutic agents that may effectively inhibit the enzyme's actions in normal subjects. The naturally occurring biflavonoids formed important hydrogen bonds, water bridges, and hydrophobic interactions with the amino acid residues of the enzyme throughout the 100 ns simulation period. Also, the DFT, RMSD, and RMSF plots showed that all the selected hit molecules were reasonably stable in the enzyme's binding pocket. Additionally, the biflavonoids showed good bioavailability and pharmacokinetic properties compared to the reference drugs. Also, the density functional theory calculations identified the biflavonoids as potential inhibitors against influenza NA. The inhibitory potential of the selected biflavonoids can be further substantiated through *in vitro* and *in vivo* pharmacological studies.

Acknowledgment: The authors gratefully acknowledge the Researchers Supporting Project (grant no. RSPD2024R885), King Saud University (Riyadh, Saudi Arabia) for supporting this work.

Funding information: No fund was received for the study.

Author contributions: Kolade O. Faloye: writing – review and editing, writing – original draft, visualization, validation, methodology, supervision, investigation, data curation, conceptualization. Shaban Ahmad: writing – review and editing, writing – original draft, visualization, validation, methodology, supervision, investigation, data curation. Olubunmi T. Oyasowo: investigation, writing – original draft. Esther O. Shalom: writing – original draft, investigation. Nagmi Bano: methodology, investigation. Esther A. Olanudun: investigation, writing – review and editing. Tawakalit O. Kelani: investigation, writing – review and editing. Habeeb. O. Aliyu: methodology. Khalid Raza: supervision, investigation, methodology, writing – review and editing. Boluwaji O. Makinde: methodology, writing – review and editing.

Conflict of interest: The authors declare that they have no known competing interest.

Ethical approval: The conducted research is not related to either human or animal use.

Data availability statement: All data generated or analyzed during this study are included in this published article and its supplementary information file.

References

[1] Wiley CA. Emergent viral infections of the CNS. J Neuropathol Exp Neurol. 2020;79(8):823–42.

[2] Hu Q, Liang W, Yi Q, Zheng Y, Wang W, Wu Y. Risk factors for death associated with severe influenza in children and the impact of the COVID-19 pandemic on clinical characteristics. Front Pediatrics. 2023;11:1–10.
[3] Zang Y, Hao D, Wang H, Yang Z, Liu H, Zhang S. Structure-based methoxyflavone derivatives with potent inhibitory activity against various influenza neuraminidases. J Biomol Struct Dyn. 2020;38(15):4617–24.
[4] Byrd-Leotis L, Cummings RD, Steinhauer DA. The interplay between the host receptor and influenza virus hemagglutinin and neuraminidase. Int J Mol Sci. 2017;18(7):1541.
[5] Guo H, Rabouw H, Slomp A, Dai M, van der Vegt F, van Lent JW, et al. Kinetic analysis of the influenza A virus HA/NA balance reveals contribution of NA to virus-receptor binding and NA-dependent rolling on receptor-containing surfaces. PLoS Pathog. 2018;14(8):e1007233.
[6] Lowe C. Viral clouds: becoming H5N1 in Indonesia. Cult Anthropol. 2010;25(4):625–49.
[7] Magano J. Synthetic approaches to the neuraminidase inhibitors zanamivir (Relenza) and oseltamivir phosphate (Tamiflu) for the treatment of influenza. Chem Rev. 2009;109(9):4398–438.
[8] Shie JJ, Fang JM. Phosphonate Congeners of Oseltamivir and Zanamivir as Effective Anti-influenza Drugs: Design, Synthesis and Biological Activity. J Chin Chem Soc. 2014;61(1):127–41.
[9] Wang K, Zhang H, Tian Y. The current strategies of optimisation of oseltamivir against mutant neuraminidases of influenza A: a review. Eur J Med Chem. 2022;243:114711.
[10] Beigel JH, Hayden FG. Influenza therapeutics in clinical practice – challenges and recent advances. Cold Spring Harb Perspect Med. 2021;11(4):1–28.
[11] Lin LT, Hsu WC, Lin CC. Antiviral natural products and herbal medicines. J Tradit Complementary Med. 2014;4(1):24–35.
[12] Musarra-Pizzo M, Pennisi R, Ben-Amor I, Mandalari G, Sciortino MT. Antiviral activity exerted by natural products against human viruses. Viruses. 2021;13(5):828.
[13] Najmi A, Javed SA, Al Bratty M, Alhazmi HA. Modern approaches in the discovery and development of plant-based natural products and their analogues as potential therapeutic agents. Molecules. 2022;27(2):349.
[14] Gontijo VS, Dos Santos MH, Viegas Jr C. Biological and chemical aspects of natural biflavonoids from plants: a brief review. Mini Rev Med Chem. 2017;17(10):834–62.
[15] Goossens JF, Goossens L, Bailly C. Hinokiflavone and related C–O–C-type biflavonoids as anticancer compounds: properties and mechanism of action. Nat Products Bioprospect. 2021;11:365–77.
[16] Mead JR, McNair N. Antiparasitic activity of flavonoids and isoflavones against Cryptosporidium parvum and Encephalitozoon intestinalis. FEMS Microbiol Lett. 2006;259(1):153–7.
[17] Shim SY, Lee SG, Lee M. Biflavonoids isolated from Selaginella tamariscina and their anti-inflammatory activities via ERK 1/2 signaling. Molecules. 2018;23(4):926.
[18] Huang W, Liu C, Liu F, Liu Z, Lai G, Yi J. Hinokiflavone induces apoptosis and inhibits migration of breast cancer cells via EMT signalling pathway. Cell Biochem Funct. 2020;38(3):249–56.
[19] Lin YM, Anderson M, Flavin MT, Pai YHS, Mata-Greenwood E, Pengsuparp T, et al. In vitro anti-HIV activity of biflavonoids isolated from Rhus succedanea and Garcinia multiflora. J Nat Products. 1997;60(9):884–8.
[20] Weniger B, Vonthron-Sénécheau C, Arango GJ, Kaiser M, Brun R, Anton R. A bioactive biflavonoid from Campnosperma panamense. Fitoterapia. 2004;75(7–8):764–7.
[21] AETih AE, Ghogomu RT, Sondengam BL, Caux C, Bodo B. Minor Biflavonoids from Lophira a lata Leaves. J Nat products. 2006;69(8):1206–8.
[22] Zhang GG, Jing Y, Zhang HM, Ma EL, Guan J, Xue FN, et al. Isolation and cytotoxic activity of selaginellin derivatives and biflavonoids from Selaginella tamariscina. Planta Medica. 2012;78(4):390–2.
[23] Šamec D, Karalija E, Dahija S, Hassan ST. Biflavonoids: Important contributions to the health benefits of Ginkgo (Ginkgo biloba L.). Plants. 2022;11(10):1381.
[24] Owoseeni OD, Patil RB, Phage PM, Ogboye RM, Ayoola MD, Famuyiwa SO, et al. Computational assessment of xanthones from African medicinal plants as aldose reductase inhibitors. Computation. 2022;10(9):146.
[25] Faloye KO, Tripathi MK, Adesida SA, Oguntimehin SA, Oyetunde YM, et al. Antimalarial potential, LC–MS secondary metabolite profiling and computational studies of Zingiber officinale. J Biomol Struct Dyn. 2024;42(5):2570–85.
[26] Famuyiwa SO, Ahmad S, Fakola EG, Olusola AJ, Adesida SA, Obagunle FO, et al. Comprehensive computational studies of naturally occurring kuguacins as antidiabetic agents by targeting visfatin. Chem Afr. 2023;6:1–13.
[27] Badshah SL, Faisal S, Muhammad A, Poulson BG, Emwas AH, Jaremko M. Antiviral activities of flavonoids. Biomed Pharmacother. 2021;140:111596.
[28] Lalani S, Poh CL. Flavonoids as antiviral agents for Enterovirus A71 (EV-A71). Viruses. 2020;12(2):184.
[29] Vavricka CJ, Li Q, Wu Y, Qi J, Wang M, Liu Y, et al. Structural and functional analysis of laninamivir and its octanoate prodrug reveals group specific mechanisms for influenza NA inhibition. PLoS Pathog. 2011;7(10):e1002249.
[30] Trott O, Olson AJ. AutoDock Vina: improving the speed and accuracy of docking with a new scoring function, efficient optimization, and multithreading. J Comput Chem. 2010;31(2):455–61.
[31] Ahmad S, Sayeed S, Bano N, Sheikh K, Raza K. In-silico analysis reveals Quinic acid as a multitargeted inhibitor against Cervical Cancer. J Biomol Struct Dyn. 2023;41(19):9770–86.
[32] Alzamami A, Alturki NA, Alghamdi YS, Ahmad S, Alshamrani S, Asiri SA, et al. Hemi-Babim and fenoterol as potential inhibitors of MPro and papain-like protease against SARS-CoV-2: an in-silico study. Medicina. 2022;58(4):515.
[33] Yadav MK, Ahmad S, Raza K, Kumar S, Eswaran M, Pasha Km M. Predictive modeling and therapeutic repurposing of natural compounds against the receptor-binding domain of SARS-CoV-2. J Biomol Struct Dyn. 2023;41(5):1527–39.
[34] Becke AD. A new mixing of Hartree–Fock and local densityfunctional theories. J Chem Phys. 1993;98(2):137.
[35] Schrödinger Release 2023–1: Maestro, Schrödinger, LLC, New York, NY, 2021.
[36] Ahmad S, Raza K. Identification of 5-nitroindazole as a multitargeted inhibitor for CDK and transferase kinase in lung cancer: a multisampling algorithm-based structural study. Mol Diversity. 2023;12(6):1–14.
[37] Ahmad S, Singh V, Gautam HK, Raza K. Multisampling-based docking reveals Imidazolidinyl urea as a multitargeted inhibitor for lung cancer: an optimisation followed multi-simulation and in-vitro study. J Biomol Struct Dyn. 2023;42(5):1–18.

[38] Ogboye RM, Patil RB, Famuyiwa SO, Faloye KO. Novel α-amylase and α-glucosidase inhibitors from selected Nigerian antidiabetic plants: an in silico approach. J Biomol Struct Dyn. 2022;40(14):6340–9.
[39] Subramanian N, Sundaraganesan N, Jayabharathi J. Molecular structure, spectroscopic (FT-IR, FT-Raman, NMR, UV) studies and first-order molecular hyperpolarizabilities of 1, 2-bis (3-methoxy-4-hydroxybenzylidene) hydrazine by density functional method. Spectrochim Acta Part A: Mol Biomol Spectrosc. 2010;76(2):259–69.
[40] Stefaniu A, Pintilie L. Molecular descriptors and properties of organic molecules. Symmetry (group theory) and mathematical treatment in chemistry. InTech, Rijeka; 2018. p. 161–76.
[41] Ayeni AO, Akinyele OF, Hosten EC, Fakola EG, Olalere JT, Egharevba GO, et al. Synthesis, crystal structure, experimental and theoretical studies of corrosion inhibition of 2-((4-(2-hydroxy-4-methylbenzyl) piperazin-1-yl) methyl)-5-methylphenol–A Mannich base. J Mol Structure. 2020;1219:128539.
[42] Srivastava K, Shimpi MR, Srivastava A, Tandon P, Sinha K, Velaga SP. Vibrational analysis and chemical activity of paracetamol–oxalic acid cocrystal based on monomer and dimer calculations: DFT and AIM approach. RSC Adv. 2016;6(12):10024–37.
[43] Domingo LR, Ríos-Gutiérrez M, Pérez P. Applications of the conceptual density functional theory indices to organic chemistry reactivity. Molecules. 2016;21(6):748.
[44] Sarukhanyan E, Shanmugam TA, Dandekar T. In silico studies reveal Peramivir and Zanamivir as an optimal drug treatment even if H7N9 avian type influenza virus acquires further resistance. Molecules. 2022;27(18):5920.
[45] Borau MS, Stertz S. Entry of influenza A virus into host cells – Recent progress and remaining challenges. Curr OpVirology. 2021;48:23–9.
[46] Matrosovich M, Herrler G, Klenk HD. Sialic acid receptors of viruses. Sialoglyco Chem Biol II: Tools Tech Identify Capture Sialoglycans. 2015;32:1–28.
[47] McAuley JL, Gilbertson BP, Trifkovic S, Brown LE, McKimm-Breschkin JL. Influenza virus neuraminidase structure and functions. Front Microbiol. 2019;10:39.
[48] Burzyńska P, Sobala LF, Mikołajczyk K, Jodłowska M, Jaśkiewicz E. Sialic acids as receptors for pathogens. Biomolecules. 2021;11(6):831.
[49] Murali KS, Sivasubramanian S, Vincent S, Murugan SB, Giridaran B, Dinesh S, et al. Anti – chikungunya activity of luteolin and apigenin rich fraction from Cynodon dactylon. Asian Pac J Trop Med. 2015;8(5):352–8.
[50] Fan W, Qian S, Qian P, Li X. Antiviral activity of luteolin against Japanese encephalitis virus. Virus Res. 2016;220:112–6.
[51] Men X, Li S, Cai X, Fu L, Shao Y, Zhu Y. Antiviral activity of luteolin against Pseudorabies virus in vitro and in vivo. Animals. 2023;13(4):761.
[52] Vacca GM, Stocco G, Dettori ML, Pira E, Bittante G, Verma NK, et al. In silico evaluation of selected flavonoids as neuraminidase inhibitors: Hope for the discovery of anti-avian influenza virus compounds. Infrared Spectrosc. 2021;104(4):3956–69.